Photo-Fenton treatment of saccharin in a solar pilot compound parabolic collector: Use of olive mill wastewater as iron chelating agent

Photo-Fenton treatment of saccharin in a solar pilot compound parabolic collector: Use of olive mill wastewater as iron chelating agent, preliminary results.

K. Davididou[a], E. Chatzisymeon[a], L. Perez-Estrada[b,c], I. Oller[b,c], S. Malato[b,c,*]

[a] School of Engineering, Institute for Infrastructure and Environment, The University of Edinburgh, Edinburgh EH9 3JL, United Kingdom

[b] Plataforma Solar de Almeria – CIEMAT, Carretera de Senés, km 4, 04200 Tabernas, Spain

[c] CIESOL, Joint Centre of the University of Almería-CIEMAT, 04120 Almería, Spain

*Corresponding author: Email: sixto.malato@psa.es; Tel.: +34950387940, fax: +34950365015

Abstract

The aim of this work was to investigate the treatment of the artificial sweetener saccharin (SAC) in a solar compound parabolic collector pilot plant by means of the photo-Fenton process at pH 2.8. Olive mill wastewater (OMW) was used as iron chelating agent to avoid acidification of water at pH 2.8. For comparative purposes, Ethylenediamine-N, N-disuccinic acid (EDDS), a well-studied iron chelator, was also employed at circumneutral pH. Degradation products formed along treatment were identified by LC-QTOF-MS analysis. Their degradation was associated with toxicity removal, evaluated by monitoring changes in the bioluminescence of *Vibrio fischeri* bacteria. Results showed that conventional photo-Fenton at pH 2.8 could easily degrade SAC and its intermediates yielding *k*, apparent reaction rate constant, in the range of 0.64-0.82 L kJ^{-1}, as well as, eliminate effluent's chronic toxicity. Both OMW and EDDS formed iron-complexes able to catalyse H_2O_2 decomposition and generate $HO^{\bullet}$. OMW yielded lower SAC oxidation rates (k=0.05-0.1 L kJ^{-1}) than EDDS (k=2.21-7.88 L kJ^{-1}) possibly due to its higher TOC contribution. However, the degradation rates were improved (k=0.13 L kJ^{-1}) by increasing OMW dilution in the reactant mixture. All in all, encouraging results were obtained by using OMW as iron chelating agent, thus rendering this approach promising towards the increase of process sustainability.

Keywords: Advanced oxidation processes (AOPs); photocatalysis; acute and chronic toxicity; iron complexes; persistent organic pollutants (POPs)

1 Introduction

Artificial sweeteners (ASs) are a new class of emerging microcontaminants with increased environmental persistence and widespread detection in the aqueous environment [1]. ASs are used increasingly worldwide as low-calorie or calorie-free sugar substitutes in food, beverages, personal care products and pharmaceuticals [2]. After consumption, they usually end up in conventional biological wastewater treatment plants. These are not originally designed to treat so recalcitrant, or low-biodegradable contaminants, which escape intact and are consequently discharged to natural water bodies where they bioaccumulate [3, 4]. This fact raises important environmental concerns because of the proven formation of toxic by-products during ASs' natural attenuation, as well as, the unawareness of their long-term ecotoxicological effects [5-7]. Among several ASs, saccharin (SAC) has been widely detected in groundwater and surface water [5, 8]. To stop ASs' release into environment, new treatment methods are sought against these recalcitrant compounds being economically viable and environmentally sustainable.

The photo-Fenton process has attracted considerable attention recently due to its well-proven efficiency in the treatment of a wide range of refractory contaminants [9]. The potential use of sunlight, a free and plentiful energy source [9, 10], as irradiation source to initiate the photo-Fenton reaction is another key feature of the process. The technology's oxidative activity is based on the reactive oxygen species (mainly $HO^{\bullet}$) that are formed when ferrous iron is oxidised by hydrogen peroxide and during the photo-reduction of ferric iron, (Eq. (1) and (2)):

$$Fe^{2+} + H_2O_2 \rightarrow Fe^{3+} + OH^- + HO^{\bullet} \quad (1)$$

$$Fe^{3+} + H_2O + hv \rightarrow Fe^{2+} + HO^{\bullet} + H^+ \quad (2)$$

The process is pH dependent (optimal pH 2.8) due to the speciation of Fe(III) and therefore strict pH control is required (acidification of the influent and later neutralisation of the effluent). Despite photo-Fenton's effectiveness to degrade recalcitrant contaminants, the additional cost of chemicals and the increased salinity of the effluent because of pH adjustments, inhibit its wide application [11]. In this respect, iron chelating agents can be used to solubilize iron in an extended pH range [12]. These chelating agents complex with iron and upon illumination via ligand-to-metal charge transfer (LCMT) reactions form photo-active species thus keeping iron in solution according to Eq. (3) [13].

$$[Fe^{3+}L]+hv\rightarrow[Fe^{3+}L]^{*}\rightarrow Fe^{2+}+L^{\bullet} \quad (3)$$

Several iron chelating agents, such as oxalate, citrate, EDDS (Ethylenediamine-N, N-disuccinic acid) and EDTA (Ethylenediaminetetraacetic acid) have been studied so far [14]. The addition of these chemical reagents in the wastewater though can substantially increase the operational cost of the process. Also, the high recalcitrance and increased toxicity [14] of such chemicals pose an environmental threat when it comes to the effluent's reuse or safe discharge.

In this view, efforts have been made to evaluate the potential of components already present in natural waters for stabilizing photo-Fenton at near-neutral pH [15]. We have already explored the use of cork boiling wastewater, a stream high in polyphenolics, in this direction [16]. Phenolic compounds are secondary plant metabolites with strong antioxidant activity based on chain-breaking and metal-chelation [17]. Such phenolic/polyphenolic components can be sourced from wastewater; in specific, they constitute a significant fraction of industrial wastewaters originating from natural products processing (i.e. cork production industry, olive mills, wineries, tea-manufacturing industry etc.), making their use in photo-Fenton treatment an economically attractive strategy. Although polyphenols such as gallic acid and tannins

have been studied as model pollutants in these waste streams, their capacity to form stable complexes with iron has not been evaluated yet [18]. It is known that among these wastewaters olive mill wastewater (OMW) features one of the highest phenolic contents (in the range of grams per litre) [19]. OMW, in specific, contains high amounts of hydroxytyrosol and gallic acid with proven iron-chelating properties at neutral pH [12, 20, 21] and for that reason is assessed here as iron chelator for the photo-Fenton process.

On this basis, the present work investigates the treatment of SAC, the forerunner of ASs, by the photo-Fenton process in a pilot-scale solar compound parabolic collector (CPC). The potential of polyphenols, present in OMW, to act as iron chelators in photo-Fenton reaction, without water acidification at pH 2.8, is evaluated. Furthermore, EDDS, known for its ability to form photoactive iron-complexes, is also used at circumneutral pH for comparison. The degradation products (DPs) formed along conventional photo-Fenton (pH 2.8) are identified and linked to toxicity evolution. To the best of our knowledge, this is the first study assessing OMW as iron chelating agent for the photo-Fenton treatment technology.

2 Materials and methods

2.1 Chemicals

SAC (98% purity, CAS No: 81-07-2) was obtained from Sigma-Aldrich. For chromatographic analysis, HPLC-grade acetonitrile and formic acid were supplied by Sigma-Aldrich. For photo-Fenton at pH 2.8, iron sulfate heptahydrate ($FeSO_4 \cdot 7H_2O$) and hydrogen peroxide (30% w/w) were obtained from Panreac. For photo-Fenton at circumneutral pH, the iron source $Fe_2(SO_4)_3 \cdot H_2O$ (75% purity) was purchased from Panreac and (S,S)-Ethylenediamine-N,N'-dissucinic acid trisodium salt solution (35% w/v) from Sigma-Aldrich. The experiments were performed using deionised water (DI, conductivity < 10 μS cm^{-1},

organic carbon < 0.5 mg L^{-1}) or natural water supplied by the Plataforma Solar de Almería (300-450 mg L^{-1} Na^{+}, 5-10 mg L^{-1} K^{+}, 30-50 mg L^{-1} Mg^{2+}, 80-120 mg L^{-1} Ca^{2+}, 250-300 mg L^{-1} SO_4^{2-}, 250-350 mg L^{-1} Cl^{-}, organic carbon < 1.0 mg L^{-1}).

2.2 Olive mill wastewater

OMW was provided by an olive mill in Andalucía (Spain) and was stored in 4^{o}C. OMW had an initial pH of 4.2, TOC (total organic carbon) =12 g L^{-1} and its polyphenolic content was 6.2 g L^{-1}.

2.3 Experimental set-up and procedure

Preliminary experiments were performed in a solar simulator (SunTest XLS+, Atlas). Irradiation was provided by a Xe lamp with an average UV irradiance of 35 W m^{-2}. Irradiance was monitored during the experiment with a SOLARLIGHT PMA2100 radiometer, placed inside the simulator. In a typical run, 1 L of SAC solution, adjusted to pH 2.8 with H_2SO_4, was loaded in a cylindrical Pyrex glass reactor (height 8.5 cm, diameter 19 cm, wall thickness 3.2 mm). The reactor was then placed inside the simulator and the desired amount of Fe and H_2O_2 were added. Solar photo-Fenton was initiated by switching on the lamp. During the experiment, the reactant mixture was continuously stirred magnetically and samples were taken at regular time intervals.

The pilot scale experiments were carried out in a 39 L CPC plant (3 m^2 total illuminated area), installed at Plataforma Solar de Almería (Tabernas Desert, Almería: latitude 37°84′N; longitude 2°34′W; altitude 500 m). The CPC plant consisted of 12 borosilicate tubes (30.0 mm inner diameter, 31.8 mm outer diameter, 1.41 m length), solar reflectors (anodized aluminium with a concentration factor of 1), a recirculation tank, a centrifugal pump, connecting tubes and valves. The schematic of the pilot plant can be found in Lapertot et al.

(2006) [22]. The illuminated area of CPC varied from 3 to 0.75 m^2, between experiments, by covering part of it. This enabled the reduction of the experimental reaction rates, allowing for a proper evaluation of intermediates formation and toxicity assessment. For experiments at pH 2.8, the pH of the DI or natural water was initially fixed with H_2SO_4. SAC solution, Fe and H_2O_2 were then added in the recirculation tank and pumped into the tubes while the reactor was covered. Similarly, for the experiments without water acidification, SAC solution, Fe:EDDS (or OMW followed by Fe) and then H_2O_2 were added and the system was left to recirculate. Fe:EDDS complexes were prepared prior to each experiment by dissolving $Fe_2(SO_4)_3 \cdot H_2O$ in 30–40 mL of distilled water acidified at pH 3 and then adding EDDS solution. In the experimental series for DPs identification and toxicity assessment, H_2O_2 was added in doses of 1 mg L^{-1} during the experiment. This method was applied to ensure that there is no residual H_2O_2 in the collected samples that could oxidise SAC and/or DPs or affect the *Vibrio fischeri* bacteria. Solar photo-Fenton was initiated by uncovering the reactor and samples were collected at predetermined times.

Experiments with different illuminated areas are comparable with each other by using Eq. (4). The plant was tilted 37°, equally to the local latitude, and a radiometer (CUV3 Model, Kipp & Zonen) equally tilted provided the global (direct + diffuse) UV radiation data. To compare the efficiency of the two reactors of different geometry and size and to include the daily variation of solar irradiation in the CPC pilot plant, the photocatalytic removal of SAC is presented as a function of the accumulated UV energy, Eq. (4):

$$Q_{UV,n+1} = Q_{UV} + \Delta t_n \cdot \overline{UV}_{G,n+1} \cdot \frac{A_i}{V_T};\ \Delta t_n = t_{n+1} - t_n \quad (4)$$

where Q_{UV} (kJ L^{-1}) is the accumulated UV energy per unit of volume, $\overline{UV}_{G,n+1}$ (W m^{-2}) is the average solar UV radiation (λ<400 nm) measured between t_{n+1} and t_n, A_i (m^2) is the

illuminated area and V_T (L) is the total volume of the reactor. In the solar simulator, UV irradiance was constant at 35 W m^{-2}.

Blank experiments revealed SAC's stability against hydrolysis and photolysis in both DI and natural water.

2.4 HPLC, TOC, spectrophotometric and toxicity analyses

The samples were filtrated with 0.2 μm hydrophobic polytetrafluoroethylene (PTFE) Millipore filters prior to chromatographic and TOC analysis. SAC concentration in filtrate samples was monitored with an Agilent 1100 series high performance liquid chromatography (HPLC). Separation was performed on a reverse phase C18 analytical column (Luna Phenomenex 5u, 150 mm x 3 mm). The mobile phase was a mixture of Milli-Q water with 0.1% formic acid and acetonitrile at 90/10 ratio that was eluted isocratically at a flow rate of 1 mL min^{-1}. The detection wavelength was set at 216 nm and the injection volume at 40 μL.

A Shimadzu TOC-V_{CSN} analyser was used for the measurement of total organic carbon. Total iron concentration was estimated by complexation with 1,10-Phenanthroline and absorbance measurement at 510 nm, according to ISO 6332. Hydrogen peroxide concentration was measured spectrophotometrically using titanium(IV) oxysulfate following the DIN 38409 H15 Standard.

Acute and chronic toxicity were evaluated by monitoring changes in the bioluminescence of *Vibrio fischeri* bacteria, in accordance with DIN EN ISO 11348-3. Prior to toxicity analysis, the pH of the samples was adjusted to 6-8 and the salinity to 2% NaCl. A BioFix Lumi-10 (Macherey-Nagel) luminometer was used for toxicity determination and the data, as presented in this study, are based on the inhibition observed at 30 min and 24 h.

2.5 LC-HRMS analysis and identification of degradation products

Liquid chromatography-mass spectrometry (LC-MS) analysis was performed in an ultra HPLC (UHPLC) Agilent 1260 Infinity system (Agilent Technologies, USA) coupled with a high resolution (HR) quadrupole time-of-flight mass spectrometer (QTOF-MS), Triple TOF 5600+ System (AB SCIEX, Concord, ON, Canada). The chromatographic separation was performed using an Agilent Zorbax Eclipse Plus C18 (3 x 150 mm, 5µm) analytical column. The mobile phases A: Milli-Q water with 0.1% formic acid and B: acetonitrile were eluted with a linear gradient starting with 10% B (2 min) and increasing to 100% B in 15 min, where it was held for 3 min before the post-column re-equilibration of 2 min. The flow rate was fixed at 0.5 mL min^{-1} and the injection volume was 50 µL.

The LC system was connected to the HRMS by a DuoSpray™ ion source, used in negative electrospray ionisation (ESI) mode. The equipment worked via TOF-MS survey scan followed by IDA (Information Dependent Acquisition). Scanned mass range was from m/z = 50 to 600 Da. IDA criteria considered dynamic background subtraction and, for MS/MS fragmentation for the four most intense ions, a collision energy of 30±15 V spread was used. Accurate mass measurements of each peak were obtained with an automated calibrant delivery system (CDS) using 0.3 mL min^{-1} of negative calibrating solution (AB Sciex). The calibration of the HRMS system was done daily and automatically after five injections. To process the HRMS data files and for DPs identification purposes, three AB Sciex software packages (Analyst® TF 1.7.1, PeakView® 2.2, MasterView® 1.1) were used.

3 Results and discussion

3.1 Conventional photo-Fenton (pH 2.8)

Preliminary experiments were carried out in the solar simulator to investigate the efficiency of conventional photo-Fenton for SAC treatment and tune the experimental protocol at low

scale. The pH of natural water was adjusted to 2.8 and left uncontrolled, no variations were observed and at the end of the experiment the measured pH was around 2.9. As seen in Figure 1, SAC was totally degraded by photo-Fenton, attaining 90% degradation when about 0.5 kJ L^{-1} of UV energy were received, approx. within 10 minutes. The process was then up-scaled to the solar CPC pilot plant, at the same photocatalytic conditions, where a slightly lower oxidation rate was observed (Figure 1). The respective UV energy for 90% SAC degradation in the CPC was 0.76 kJ L^{-1}, corresponding to less than 15 min of irradiation time. The observed discrepancy between the removal efficiencies is small and can be attributed to the different size and geometry of the two systems. The main conclusions drawn are that (i) the two systems could be easily compared when using Q_{UV} instead of time and (ii) Fe concentration of 5 mg L^{-1} was able to degrade SAC rapidly. All subsequent experiments were performed at pilot scale since the obtained results could be more useful for future scale-up.

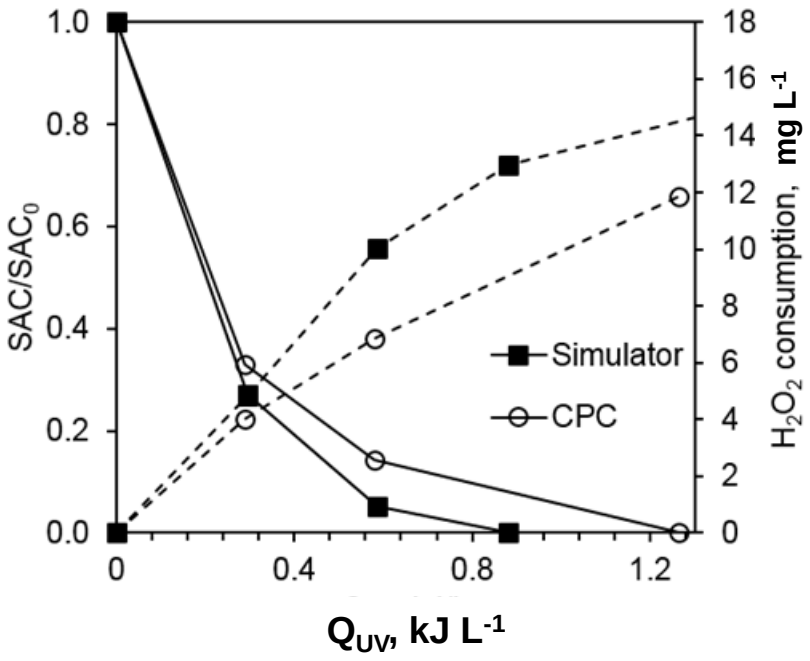

Figure 1. SAC photocatalytic degradation (solid line) and the respective H_2O_2 consumption (dashed line) in the solar simulator and CPC pilot plant. Experimental conditions: $[SAC]_0$=5 mg L^{-1}, H_2O_2=20 mg L^{-1}, Fe=5 mg L^{-1}, pH=2.8, natural water.

3.1.1 Effect of initial SAC concentration

The effect of initial SAC concentration (2.5, 5 and 10 mg L^{-1}) on its photocatalytic degradation was assessed. The concentration of Fe was reduced to 2 mg L^{-1} in order to slow down the reaction rate and thus to permit a proper evaluation of DPs formation and toxicity evolution. As presented in Figure 1, SAC degradation in the presence of 5 mg L^{-1} Fe is rapid and therefore it is difficult to trace down any information about intermediates and toxicity evolution during the first steps of treatment. Results in Figure 2 show that the reaction rate decreases with the initial concentration of SAC, implying first-order kinetics according to Eq. (5):

$$\ln\left(\frac{[SAC]}{[SAC]_0}\right) = -k\,Q_{UV,n} \qquad (5)$$

where k (L kJ^{-1}) is an apparent reaction rate constant. From the plot of normalized SAC concentration against Q_{UV}, k in the range of 0.64-0.82 ±0.05 L kJ^{-1} were obtained (the coefficient of linear regression of data fitting, r^2, is between 98.7 and 99.2%).

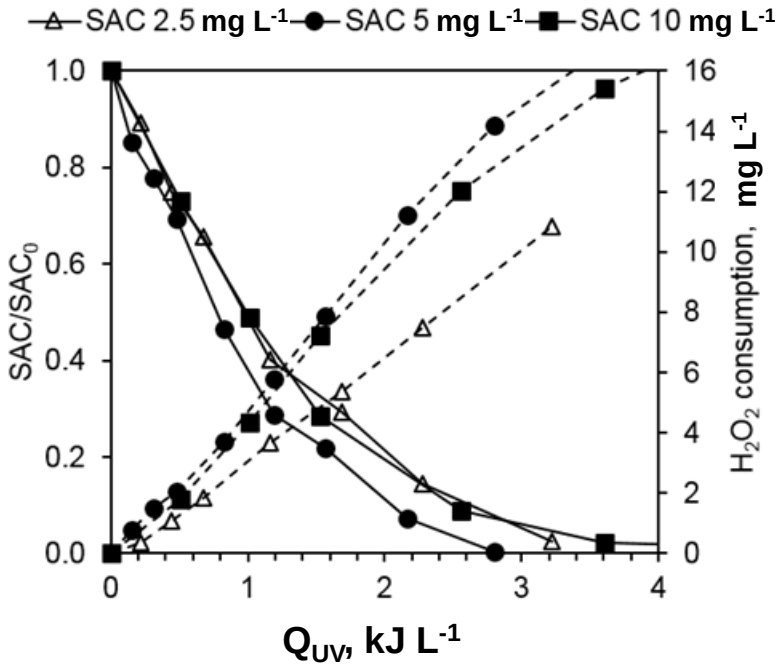

Figure 2. SAC photocatalytic degradation (solid line) and the respective H_2O_2 consumption (dashed line) at various initial SAC concentrations in the solar CPC pilot plant. Experimental conditions: H_2O_2=20 mg L^{-1}, Fe=2 mg L^{-1}, pH=2.8, natural water.

Also, in Figure 2 it can be observed that H_2O_2 consumption increases with initial SAC concentration; in detail, 8.8, 10.5 and 12 mg L^{-1} H_2O_2 are consumed to degrade 90% of 2.5, 5 and 10 mg L^{-1} of SAC, respectively. H_2O_2 is mainly consumed during the oxidation of ferrous iron (Eq. (1)), which is generated by the photo-reduction of ferric iron (Eq. (2)). Therefore, at higher initial concentration of SAC, the increased Q_{UV} requirement results in higher photo-generation of ferrous iron that corresponds to increased H_2O_2 consumption, explaining the obtained results.

3.1.2 Degradation products

LC-QTOF-MS analysis revealed the formation of nine DPs during the photocatalytic treatment of SAC with high degree of certainty (<4 ppm error). The DPs' high resolution mass spectra data are summarised in Table 1. The evolution profiles of DPs confirm the

efficiency of the photo-Fenton process to degrade them in both DI and natural water (Figures 3 and 4, respectively). Interestingly, the concentration of DP3 increases slightly with treatment in both water matrices and, in a similar way, DP3 is the last DP to evolve as in the study of Davididou et al. (2017) before its complete oxidation [23]. In natural water, DPs degradation proceeds slower than in DI water due to the various inorganic and organic species that are present and can act as $HO^{\bullet}$ scavengers [11].

The generated DPs are formed by different types of isomers, following a degradation pathway previously reported in Davididou et al. (2017) and their proposed molecular structures are shown in Table 2 [23].

Table 1. High resolution mass spectra data of the identified DPs. Experimental conditions: $[SAC]_0$=10 mg L^{-1}, Fe=2 mg L^{-1}, pH=2.8.

t_R (min)	**Code name**	**Elemental composition (deprotonated molecule)**	**Calculated exact mass $[M-H]^-$**	**Detected exact mass $[M-H]^-$**	**Error (ppm)**	**DBE**	**logP[#]**
DPs in DI water							
5,54	DP1-a	$C_7H_4NO_4S^-$	197,9866	197,9851	-7,5	6,5	0,046
6,72	DP1-b	$C_7H_4NO_4S^-$	197,9866	197,986	-3	6,5	0,468
7,08	DP1-c	$C_7H_4NO_4S^-$	197,9866	197,9856	-5	6,5	0,475
11,4	DP1-d	$C_7H_4NO_4S^-$	197,9866	197,9855	-5,5	6,5	0,904
4,91	DP2-a	$C_7H_4NO_5S^-$	213,9815	213,9804	-5	6,5	-0,199 / -0,201[$]
5,52	DP2-b	$C_7H_4NO_5S^-$	213,9815	213,9802	-6	6,5	0,081
5,93	DP2-c	$C_7H_4NO_5S^-$	213,9815	213,9802	-6	6,5	0,491
6,42	DP2-d	$C_7H_4NO_5S^-$	213,9815	213,98023	-5,9	6,5	0,652
18,0	DP3	$C_7H_6NO_6S^-$	231,9920	231,99218	-0,7	5,5	
DPs in natural water							

5,54	DP1-a	$C_7H_4NO_4S^-$	197,9866	197,9869	1,24	6,5	0,046
6,72	DP1-b	$C_7H_4NO_4S^-$	197,9866	197,9872	2,76	6,5	0,468
7,08	DP1-c	$C_7H_4NO_4S^-$	197,9866	197,9874	3,77	6,5	0,475
11,4	DP1-d	$C_7H_4NO_4S^-$	197,9866	197,9869	1,24	6,5	0,904
4,91	DP2-a	$C_7H_4NO_5S^-$	213,9815	213,9808	-3,27	6,5	-0,199 / -0,201[$]
5,52	DP2-b	$C_7H_4NO_5S^-$	213,9815	213,9808	-3,27	6,5	0,081
5,93	DP2-c	$C_7H_4NO_5S^-$	213,9815	213,981	-2,33	6,5	0,491
6,42	DP2-d	$C_7H_4NO_5S^-$	213,9815	213,9804	-5,14	6,5	0,652
18	DP3	$C_7H_6NO_6S^-$	231,9920	231,9921	-0,43	5,5	

[#] Lipophilicity index (i.e., in a C18 column compounds with logP > 0 will have high retention times, and those with logP < -1 low retention times). Calculated using ACD/ChemSketch molecular properties calculator

[$] Two different isomers might be co-eluting in the same peak due to the similar logP

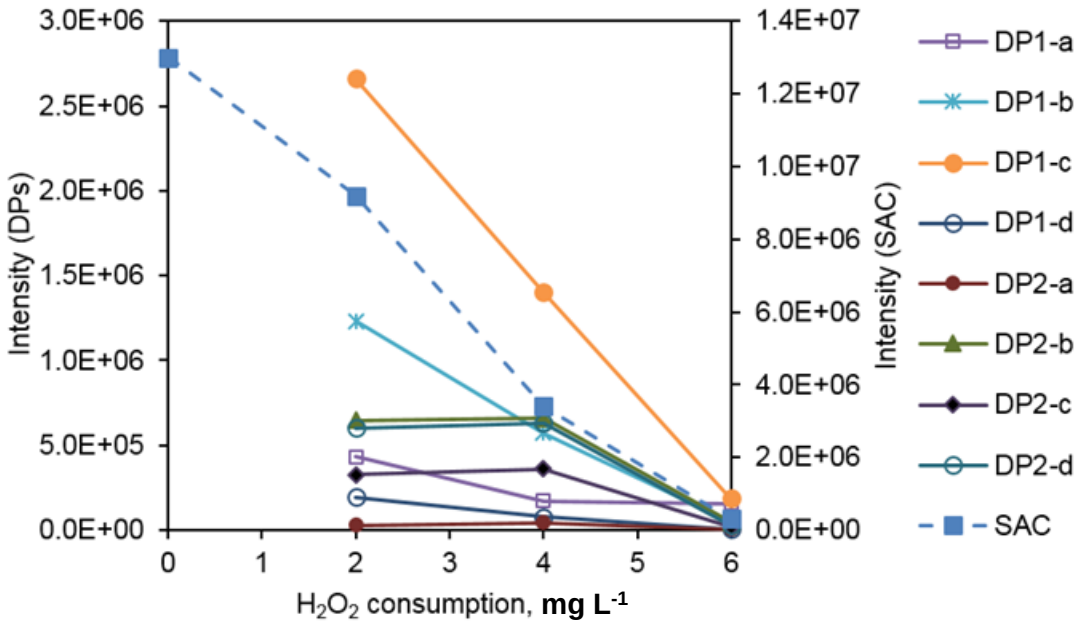

Figure 3. The kinetic profiles of SAC DPs in DI water as a function of H_2O_2 consumption. Experimental conditions: $[SAC]_0$=10 mg L^{-1}, Fe=2 mg L^{-1}, pH=2.8.

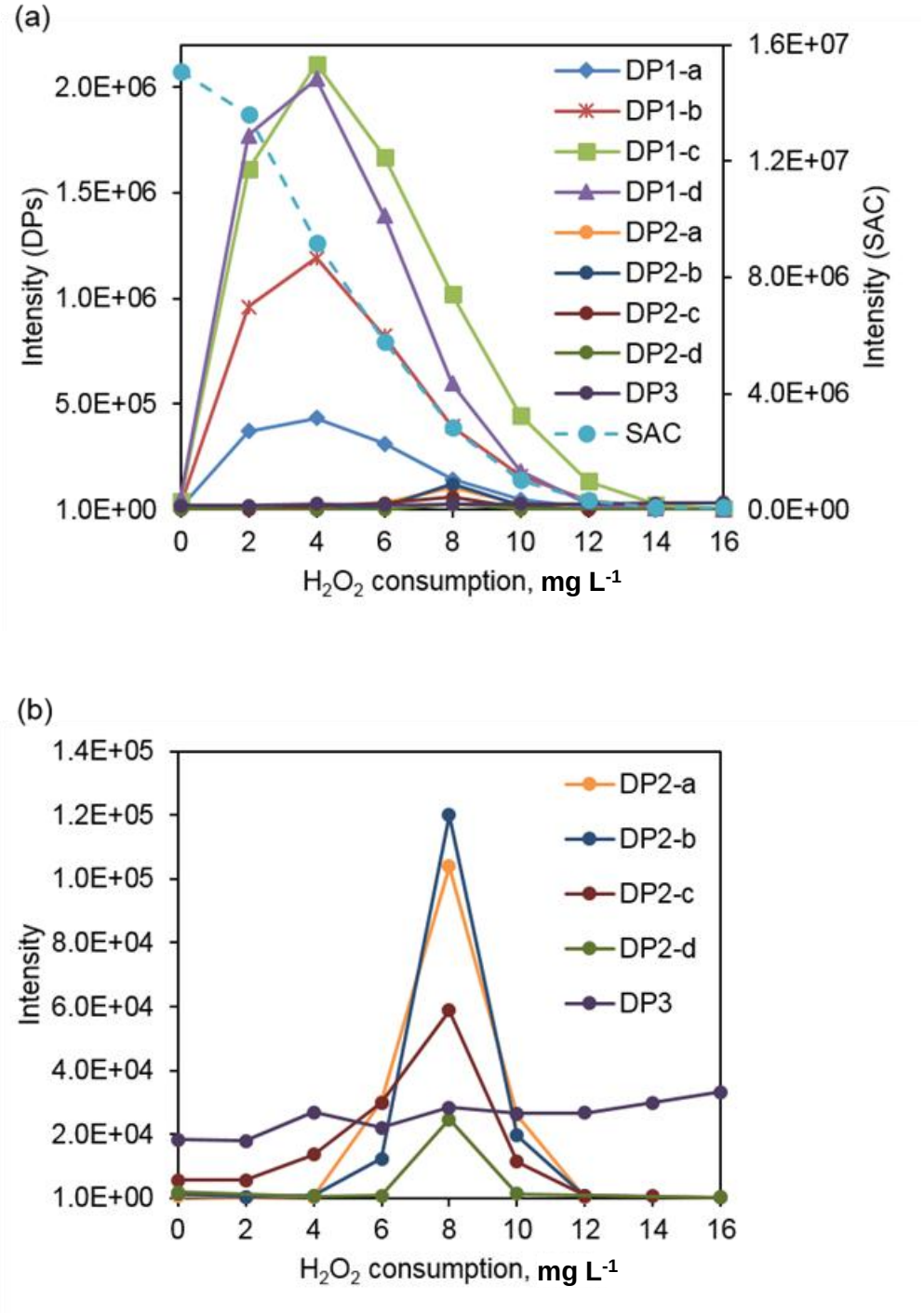

Figure 4. The kinetic profiles of (a) SAC and all the detected DPs and (b) low-intensity DPs alone in natural water as a function of H_2O_2 consumption. Experimental conditions: $[SAC]_0$=10 mg L^{-1}, Fe=2 mg L^{-1}, pH=2.8.

Table 2. Proposed molecular structures of the identified DPs derived from LC-QTOF-MS analysis.

Code name	Structure	Code name	Structure
SAC	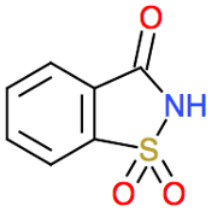	DP2-a	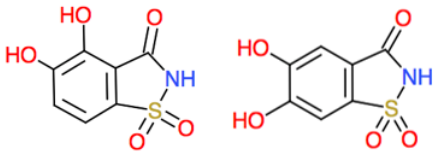 logP -0.199 logP -0.201
DP1-a	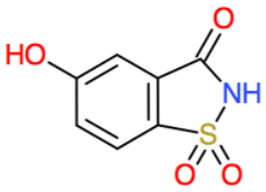	DP2-b	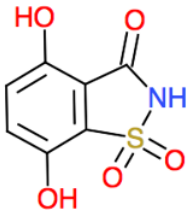
DP1-b	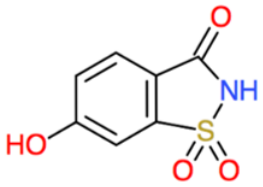	DP2-c	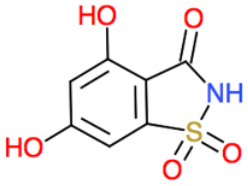
DP1-c	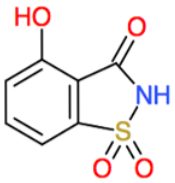	DP2-d	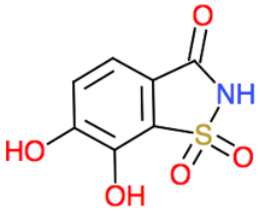
DP1-d	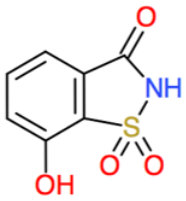	DP3	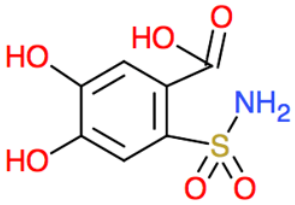

3.1.3 Toxicity assessment

The ecotoxicity evaluation of various ASs, including SAC, in their original form as food additives, has shown a low risk towards aquatic organisms (i.e. activated sewage sludge communities, green algae *Scenedesmus vacuolatus*, water fleas *Daphnia magna* and

duckweed *Lemna minor*) [24]. However, when ASs are released into the environment they undergo transformations after exposure to solar radiation and DPs more toxic than the parent compounds could be formed with adverse effects on aquatic life. Calza et al. (2013), Sang et al. (2014) and Ren et al. (2016) have confirmed toxicity photo-enhancement for the ASs sucralose and acesulfame [5, 7, 25], however the toxicity of photocatalytically treated SAC has yet to be studied.

In this direction, acute and chronic toxicity of the treated samples were evaluated by monitoring the inhibition of *Vibrio fischeri* bioluminescence. According to the acute toxicity profile (Figure 5a), the bacteria are slightly stimulated in the initial stages of photo-Fenton treatment (H_2O_2 consumption <8 mg L^{-1}); possibly indicating the ability of *Vibrio fischeri* to metabolise the main SAC intermediates, shown in Figure 4 and Table 2, more easily than SAC parent compound. After that, inhibition remains lower than 10%, suggesting that acute toxicity is very low and the solution is innocuous to *Vibrio fischeri* before, during and after treatment.

Interestingly, the results of chronic toxicity vary significantly. Exposure of *Vibrio fischeri* to the treated samples for 24 h results in rapid increase of bioluminescence inhibition (Figure 5b) that is gradually reduced along treatment. The results indicate that toxicity is linked with the presence of DPs. The highest inhibition percentages (84-93%) are measured at the maximum concentration of DPs and then decrease with DPs (Figure 4) when H_2O_2 consumption is over 8 mg L^{-1}. The connection between chronic toxicity and DPs indicates the toxic nature of the DPs formed along treatment and, furthermore, shows the efficiency of the photo-Fenton process in reducing chronic toxicity from the treated effluent. It is important to remark the difference between acute and chronic toxicity. As previously discussed, DPs could stimulate *Vibrio fischeri* bacteria after a short contact time but develop toxicity after longer

exposure periods, hence highlighting the necessity of continuing the treatment until the complete degradation of the main DPs.

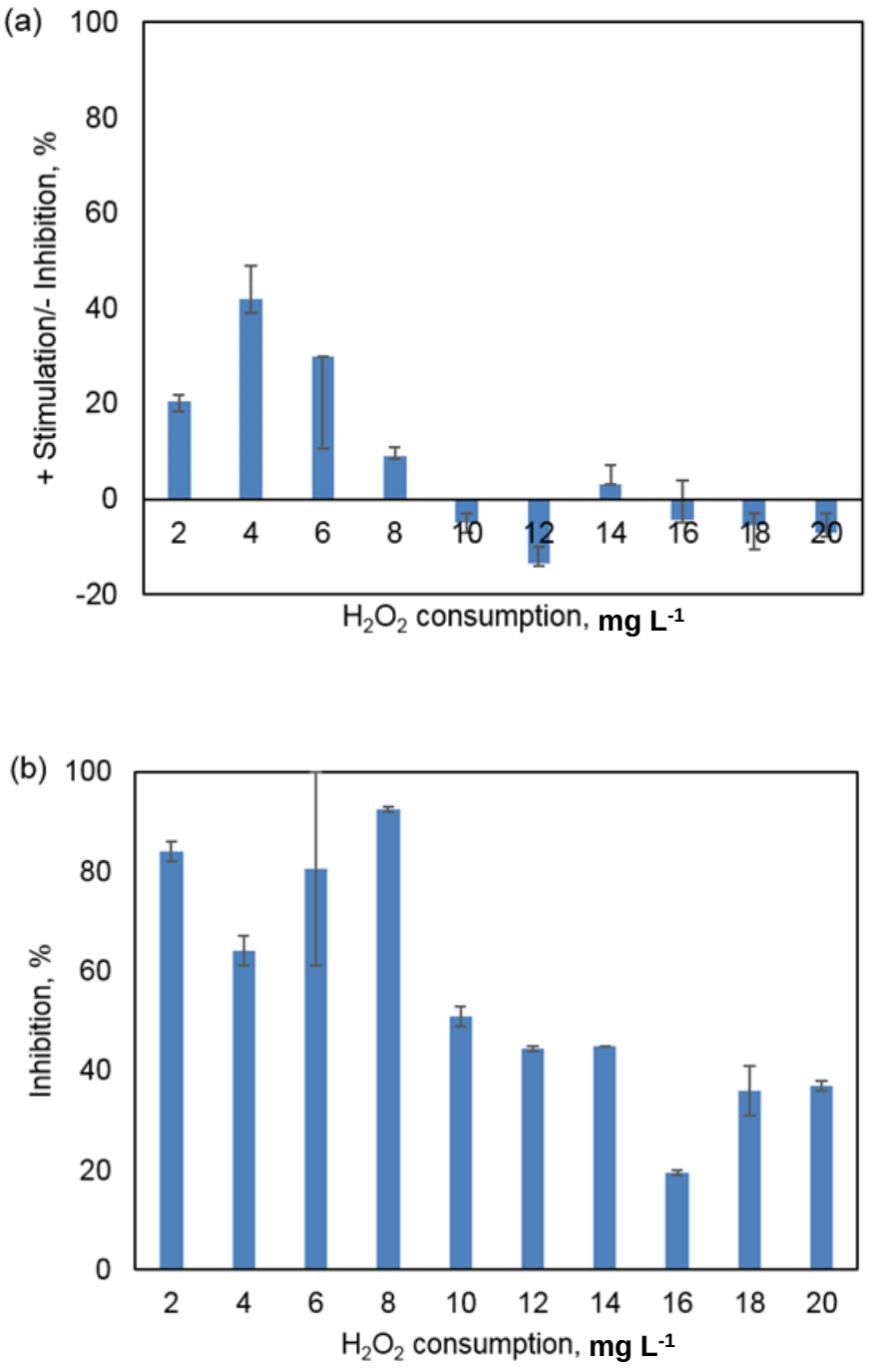

Figure 5. Inhibition of the bioluminescence of bacteria *Vibrio fischeri* as a function of H_2O_2 consumption after (a) 30 min and (b) 24 h exposure to the treated samples. Experimental conditions: $[SAC]_0$=10 mg L^{-1}, Fe=2 mg L^{-1}, pH=2.8, natural water.

3.2 EDDS assisted photo-Fenton at circumneutral pH

The photo-Fenton treatment of SAC catalysed by Fe:EDDS at circumneutral pH 5.6-5.9 was then investigated. EDDS is a well-studied iron chelating agent, non-toxic and readily biodegradable and has demonstrated the highest catalytic activity among other chelators such as EDTA, oxalate and citrate [26]. Fe:EDDS at a molar ratio 1:2 was applied, based on previous findings of Klamerth et al. (2012) [11]. The pH was found to be stable during the treatment.

The effect of initial SAC concentration on its degradation during EDDS assisted photo-Fenton was evaluated by applying various initial SAC concentrations (2.5-10 mg L^{-1}). As seen in Figure 6, removal efficiency decreases with the increase of initial SAC concentration, suggesting first-order kinetics. In detail, increase of SAC concentration from 2.5 to 10 mg L^{-1} leads to the respective *k*, reduction from 7.88 to 2.21 L kJ^{-1} (with the r^2 between 96.2 and 99.9%). Increase in the initial organic substrate concentration, at a fixed set of photocatalytic conditions, lowers the ratio of $HO^{\bullet}$ to substrate and further decreases degradation yields, thus explaining the results presented above. In Figure 6, it can be also observed that H_2O_2 consumption increases with SAC concentration; this increase is attributed to the increased UV energy requirement as described in 3.1.1. In detail, 5.1, 16.3 and 19.3 mg L^{-1} H_2O_2 are required to degrade 90% of 2.5, 5 and 10 mg L^{-1} of SAC. It is known that EDDS assisted photo-Fenton is mostly suitable for short treatment times since Fe:EDDS is photolysed leading to the depletion of EDDS and accumulation of Fe^{3+} in solution that contribute to the faster formation of insoluble Fe species [27]. Byproducts of EDDS could also compete for radical oxidixing species. This also justifies the low reaction rates observed at longer treatment times when 5 and 10 mg L^{-1} initial SAC concentration are applied.

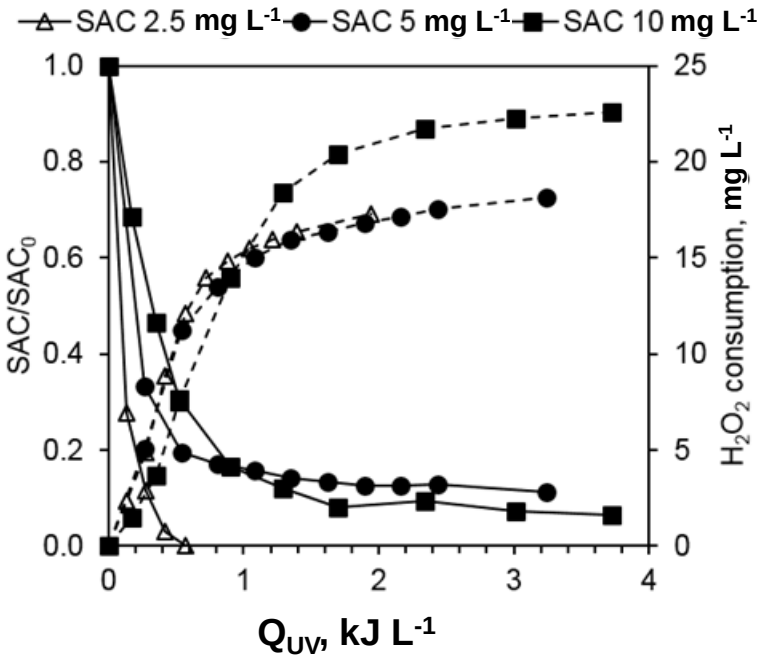

Figure 6. The effect of initial SAC concentration on its photocatalytic degradation (solid line) and the respective H_2O_2 consumption (dashed line) using 1:2 mM of Fe:EDDS in the solar CPC pilot plant. Experimental conditions: H_2O_2=20 mg L^{-1}, Fe=2 mg L^{-1}, circumneutral pH, DI water.

3.3 OMW assisted photo-Fenton (pH >4.5)

3.3.1 Effect of initial SAC concentration

The potential of OMW to form photoactive Fe^{3+} complexes, in order to avoid acidification of water at pH 2.8, was assessed. OMW was diluted 400 times in the reactant mixture (WW). Considering its organic load, the concentration of H_2O_2 was monitored throughout the experiment and was always kept > 10 mg L^{-1}, starting with an initial H_2O_2 dose of 20 mg L^{-1} and applying interim H_2O_2 additions. The pH tended to fall during treatment due to the acidic nature of SAC and OMW, therefore NaOH was added to maintain pH >4.5 and prevent SAC oxidation due to conventional photo-Fenton process.

As seen in Figure 7, SAC degradation is irrespective of the initial SAC concentration. Fe:OMW complex catalyses the decomposition of H_2O_2, leading to the generation of $HO^{\bullet}$ that oxidise SAC yielding k in the range of 0.05-0.1 L kJ^{-1} (r^2 between 93 and 99%). The low reaction yields obtained can be attributed to the competition between SAC and OMW's organics (TOC 30 mg L^{-1}) for the available $HO^{\bullet}$. Measurement of the iron concentration reveals complete chelation of the 2 mg L^{-1} Fe^{3+} and evidences the formation of stable complexes that keep iron in solution throughout the experiment. Considering the observed low oxidation rates, OMW diluted > 400 times is tested in the following experiments to reduce the organic content in the reactant mixture, while keeping SAC at 10 mg L^{-1}.

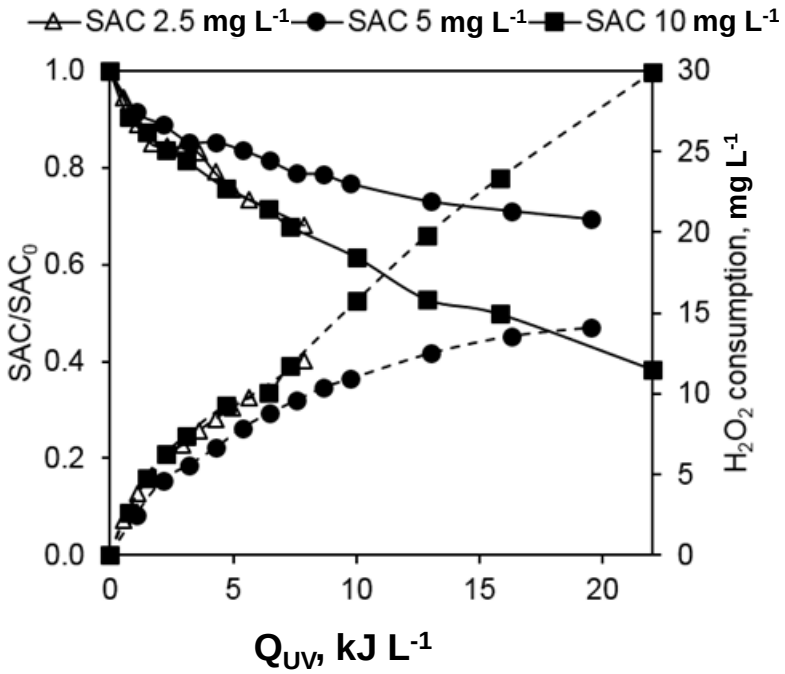

Figure 7. The effect of initial SAC concentration on its photocatalytic degradation (solid line) and the respective H_2O_2 consumption (dashed line) using OMW:WW 1:400 in the solar CPC pilot plant. Experimental conditions: $[H_2O_2]_0$=20 mg L^{-1}, Fe=2 mg L^{-1}, DI water.

3.3.2 Effect of OMW dilution

Higher OMW:WW dilutions (i.e. 1:800, 1:1000 and 1:1200) were applied for the photocatalytic degradation of SAC, as an attempt to increase removal efficiency by reducing the TOC contribution of OMW. TOC was 15, 12 and 10 mg L^{-1}, respectively. H_2O_2 concentration was maintained higher than 10 mg L^{-1} throughout the experiment with interim H_2O_2 additions, as previously. As seen in Figure 8, OMW:WW 1:800 is the ratio yielding the highest oxidation rate (k =0.13 L kJ^{-1}) and, in this case, the UV energy required for 90% SAC degradation is 13.5 kJ L^{-1}. This ratio OMW:WW was enough to keep iron in solution at lower TOC than 1:400. Higher dilutions were not able to keep enough iron in solution.

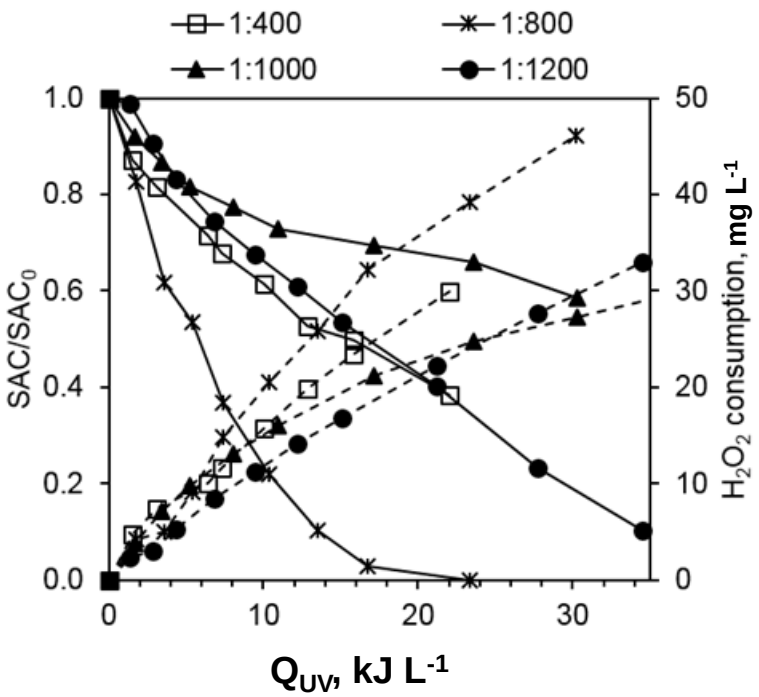

Figure 8. The effect of OMW dilution on SAC photocatalytic degradation (solid line) and the respective H_2O_2 consumption (dashed line) in the solar CPC pilot plant. Experimental conditions: $[SAC]_0$=10 mg L^{-1}, $[H_2O_2]_0$= 20 mg L^{-1}, Fe=2 mg L^{-1}, DI water.

3.4 Comparison of conventional, Fe:EDDS and Fe:OMW photo-Fenton

The efficiency of the different photo-Fenton processes, in terms of SAC removal, was found to descend in the following order: Fe:EDDS at circumneutral pH > photo-Fenton at pH 2.8 > Fe:OMW at pH over 4.5. Similar findings have been reported by Papoutsakis et al. (2015), when they compared conventional with Fe:EDDS photo-Fenton for the degradation of imidacloprid [27]. They suggested that Fe:EDDS is more photoactive than the aqua complexes formed during conventional photo-Fenton. This results in the Fe^{2+} becoming available faster for reacting with H_2O_2 meaning faster generation of $HO^{\bullet}$, which can also explain the high yields obtained by EDDS in the present study. The lowest activity was observed when OMW was used as iron chelator, possibly due to its high organic content that consumes the available $HO^{\bullet}$, which otherwise would be intended for SAC degradation.

The initial concentration of iron is maintained throughout the experiment during conventional photo-Fenton, regardless of the received UV energy. Nonetheless, when EDDS or OMW is used the photogenerated $HO^{\bullet}$ attack both SAC and chelators. As a result, iron-complexes are breaking, iron is released and subsequently precipitates, thus lowering the photocatalytic activity [27, 28]. It should be noted that in the case of EDDS, iron leaching is higher (26-33% decrease of soluble iron at a total UV energy of 1.9-3.2 kJ L^{-1}) than in the OMW assisted photo-Fenton (4-11% decrease of soluble iron at a total UV energy of 8-13 kJ L^{-1}); a fact that indicates the higher stability of the chelates and their increased resistance against $HO^{\bullet}$ and UV radiation when Fe:OMW is used.

From this point of view, the increased stability of iron chelating agents against photo-Fenton treatment is highly desirable, although overall efficiency is always important. OMW is a waste stream rich in organics and polyphenols, in the range of grams per litre, with high ecotoxicity and strong antibacterial properties [29]. However, when diluted hundreds of

times, ecotoxicity is not of concern, making it a good choice (valorisation of a waste stream) for photo-Fenton treatment of other wastewaters without pH adjustment. Besides, if properly dosed, most of its organic content including polyphenols would be degraded during the process since photo-Fenton has been found to degrade efficiently OMW and to eliminate its toxicity [30, 31].

4 Conclusions

Conventional photo-Fenton was found to be an effective method for the degradation of SAC and its DPs, as well as for the elimination of effluent's toxicity. The main DPs formed along SAC treatment were identified by means of LC-QTOF-MS and linked to chronic toxicity, as acute toxicity was negligible. OMW highly diluted (around 800 times) was assessed as an alternative to EDDS for iron chelation since iron was kept in solution and active to degrade SAC. At the conditions employed in this study, Fe:EDDS yielded the highest oxidation rates among conventional photo-Fenton and OMW assisted photo-Fenton. However, this study introduces a new concept towards the sustainable operation of photo-Fenton that is based on the use of wastewaters rich in polyphenols instead of pricey and hazardous chemicals for iron chelation.

Acknowledgements

Financial support by the FP7-Infrastructures EU Programme through the SFERA-II Grant Agreement no. 312643 is gratefully acknowledged. L.P.E. would like to thank the Ministerio de Economía, Industria y Competitividad (MINECO) for the research contract RYC-2014-15194. L.P.E., I.O and S.M wish to thank the Spanish Ministry of Economy and Competitiveness for funding under the TRICERATOPS Project (Reference: CTQ2015-

69832-C4-1-R). The authors would also like to thank Isabel Fernández, Elisa Ramos and Agustín Carrión for their help during this experimental work and Ana Belén Martínez for her help with LC-QTOF-MS.

References

[1] F.T. Lange, M. Scheurer, H.-J. Brauch, Artificial sweeteners—a recently recognized class of emerging environmental contaminants: a review, Anal. Bioanal. Chem., 403 (2012) 2503-2518.

[2] A. Zygler, A. Wasik, J. Namieśnik, Analytical methodologies for determination of artificial sweeteners in foodstuffs, TrAC, Trends Anal. Chem., 28 (2009) 1082-1102.

[3] D.R. Van Stempvoort, J.W. Roy, S.J. Brown, G. Bickerton, Artificial sweeteners as potential tracers in groundwater in urban environments, Journal of Hydrology, 401 (2011) 126-133.

[4] M. Scheurer, F.R. Storck, H.-J. Brauch, F.T. Lange, Performance of conventional multi-barrier drinking water treatment plants for the removal of four artificial sweeteners, Water Res., 44 (2010) 3573-3584.

[5] Z. Sang, Y. Jiang, Y.-K. Tsoi, K.S.-Y. Leung, Evaluating the environmental impact of artificial sweeteners: A study of their distributions, photodegradation and toxicities, Water Res., 52 (2014) 260-274.

[6] A.J. Li, O.J. Schmitz, S. Stephan, C. Lenzen, P.Y.-K. Yue, K. Li, H. Li, K.S.-Y. Leung, Photocatalytic transformation of acesulfame: Transformation products identification and embryotoxicity study, Water Res., 89 (2016) 68-75.

[7] Y. Ren, J. Geng, F. Li, H. Ren, L. Ding, K. Xu, The oxidative stress in the liver of Carassius auratus exposed to acesulfame and its UV irradiance products, Sci. Total Environ., 571 (2016) 755-762.

[8] M. Scheurer, H.-J. Brauch, F.T. Lange, Analysis and occurrence of seven artificial sweeteners in German waste water and surface water and in soil aquifer treatment (SAT), Anal. Bioanal. Chem., 394 (2009) 1585-1594.

[9] J.J. Pignatello, E. Oliveros, A. MacKay, Advanced Oxidation Processes for Organic Contaminant Destruction Based on the Fenton Reaction and Related Chemistry, Crit. Rev. Environ. Sci. Technol., 36 (2006) 1-84.

[10] S. Malato, P. Fernández-Ibáñez, M.I. Maldonado, J. Blanco, W. Gernjak, Decontamination and disinfection of water by solar photocatalysis: Recent overview and trends, Catal. Today, 147 (2009) 1-59.

[11] N. Klamerth, S. Malato, A. Agüera, A. Fernández-Alba, G. Mailhot, Treatment of Municipal Wastewater Treatment Plant Effluents with Modified Photo-Fenton As a Tertiary Treatment for the Degradation of Micro Pollutants and Disinfection, Environ. Sci. Technol., 46 (2012) 2885-2892.

[12] Y. Sun, J.J. Pignatello, Chemical treatment of pesticide wastes. Evaluation of iron(III) chelates for catalytic hydrogen peroxide oxidation of 2,4-D at circumneutral pH, Journal of Agricultural and Food Chemistry, 40 (1992) 322-327.

[13] Y. Sun, J.J. Pignatello, Activation of hydrogen peroxide by iron(III) chelates for abiotic degradation of herbicides and insecticides in water, J. Agric. Food. Chem., 41 (1993) 308-312.

[14] L. Clarizia, D. Russo, I. Di Somma, R. Marotta, R. Andreozzi, Homogeneous photo-Fenton processes at near neutral pH: A review, Applied Catalysis B: Environmental, 209 (2017) 358-371.

[15] J. Ndounla, C. Pulgarin, Evaluation of the efficiency of the photo Fenton disinfection of natural drinking water source during the rainy season in the Sahelian region, Sci. Total Environ., 493 (2014) 229-238.

[16] S. Papoutsakis, C. Pulgarin, I. Oller, R. Sánchez-Moreno, S. Malato, Enhancement of the Fenton and photo-Fenton processes by components found in wastewater from the industrial processing of natural products: The possibilities of cork boiling wastewater reuse, Chem. Eng. J., 304 (2016) 890-896.

[17] S. Khokhar, R.K. Owusu Apenten, Iron binding characteristics of phenolic compounds: some tentative structure–activity relations, Food Chem., 81 (2003) 133-140.

[18] M.S. Masoud, A.E. Ali, S.S. Haggag, N.M. Nasr, Spectroscopic studies on gallic acid and its azo derivatives and their iron(III) complexes, Spectrochimica Acta Part A: Molecular and Biomolecular Spectroscopy, 120 (2014) 505-511.

[19] L. Bertin, F. Ferri, A. Scoma, L. Marchetti, F. Fava, Recovery of high added value natural polyphenols from actual olive mill wastewater through solid phase extraction, Chem. Eng. J., 171 (2011) 1287-1293.

[20] M. Andjelković, J. Van Camp, B. De Meulenaer, G. Depaemelaere, C. Socaciu, M. Verloo, R. Verhe, Iron-chelation properties of phenolic acids bearing catechol and galloyl groups, Food Chem., 98 (2006) 23-31.

[21] N. Kalogerakis, M. Politi, S. Foteinis, E. Chatzisymeon, D. Mantzavinos, Recovery of antioxidants from olive mill wastewaters: A viable solution that promotes their overall sustainable management, J. Environ. Manage., 128 (2013) 749-758.

[22] M. Lapertot, C. Pulgarín, P. Fernández-Ibáñez, M.I. Maldonado, L. Pérez-Estrada, I. Oller, W. Gernjak, S. Malato, Enhancing biodegradability of priority substances (pesticides) by solar photo-Fenton, Water Research, 40 (2006) 1086-1094.

[23] K. Davididou, C. McRitchie, M. Antonopoulou, I. Konstantinou, E. Chatzisymeon, Photocatalytic degradation of saccharin under UV-LED and blacklight irradiation, Journal of Chemical Technology & Biotechnology, (2017) In press.

[24] S. Stolte, S. Steudte, N.H. Schebb, I. Willenberg, P. Stepnowski, Ecotoxicity of artificial sweeteners and stevioside, Environ. Int., 60 (2013) 123-127.

[25] P. Calza, V.A. Sakkas, C. Medana, A.D. Vlachou, F. Dal Bello, T.A. Albanis, Chemometric assessment and investigation of mechanism involved in photo-Fenton and TiO2 photocatalytic degradation of the artificial sweetener sucralose in aqueous media, Applied Catalysis B: Environmental, 129 (2013) 71-79.

[26] W. Huang, M. Brigante, F. Wu, K. Hanna, G. Mailhot, Development of a new homogenous photo-Fenton process using Fe(III)-EDDS complexes, Journal of Photochemistry and Photobiology A: Chemistry, 239 (2012) 17-23.

[27] S. Papoutsakis, F.F. Brites-Nóbrega, C. Pulgarin, S. Malato, Benefits and limitations of using Fe(III)-EDDS for the treatment of highly contaminated water at near-neutral pH, J. Photochem. Photobiol. A: Chem., 303 (2015) 1-7.

[28] A. De Luca, R.F. Dantas, S. Esplugas, Assessment of iron chelates efficiency for photo-Fenton at neutral pH, Water Res., 61 (2014) 232-242.

[29] E. Chatzisymeon, N.P. Xekoukoulotakis, E. Diamadopoulos, A. Katsaounis, D. Mantzavinos, Boron-doped diamond anodic treatment of olive mill wastewaters: Statistical analysis, kinetic modeling and biodegradability, Water Res., 43 (2009) 3999-4009.

[30] D. Mantzavinos, N. Kalogerakis, Treatment of olive mill effluents, Environ. Int., 31 (2005) 289-295.

[31] W. Gernjak, M.I. Maldonado, S. Malato, J. Cáceres, T. Krutzler, A. Glaser, R. Bauer, Pilot-plant treatment of olive mill wastewater (OMW) by solar TiO2 photocatalysis and solar photo-Fenton, Solar Energy, 77 (2004) 567-572.